Video Article

Optical Trapping of Nanoparticles

Jarrah Bergeron, Ana Zehtabi-Oskuie, Saeedeh Ghaffari, Yuanjie Pang, Reuven Gordon
Electrical and Computer Engineering, University of Victoria

Correspondence to: Reuven Gordon at rgordon@uvic.ca

URL: http://www.jove.com/video/4424
DOI: doi:10.3791/4424

Keywords: Physics, Issue 71, Nanotechnology, Optics, Electrical Engineering, Computer Engineering, Physical Sciences, Engineering, Plasmonics, optical trapping, dielectric nanoparticles, nanoholes, nanofabrication, nano, microfluidics

Date Published: 1/15/2013

Citation: Bergeron, J., Zehtabi-Oskuie, A., Ghaffari, S., Pang, Y., Gordon, R. Optical Trapping of Nanoparticles. *J. Vis. Exp.* (71), e4424, doi:10.3791/4424 (2013).

Abstract

Optical trapping is a technique for immobilizing and manipulating small objects in a gentle way using light, and it has been widely applied in trapping and manipulating small biological particles. Ashkin and co-workers first demonstrated optical tweezers using a single focused beam[1]. The single beam trap can be described accurately using the perturbative gradient force formulation in the case of small Rayleigh regime particles[1]. In the perturbative regime, the optical power required for trapping a particle scales as the inverse fourth power of the particle size. High optical powers can damage dielectric particles and cause heating. For instance, trapped latex spheres of 109 nm in diameter were destroyed by a 15 mW beam in 25 sec[1], which has serious implications for biological matter[2,3].

A self-induced back-action (SIBA) optical trapping was proposed to trap 50 nm polystyrene spheres in the non-perturbative regime[4]. In a non-perturbative regime, even a small particle with little permittivity contrast to the background can influence significantly the ambient electromagnetic field and induce a large optical force. As a particle enters an illuminated aperture, light transmission increases dramatically because of dielectric loading. If the particle attempts to leave the aperture, decreased transmission causes a change in momentum outwards from the hole and, by Newton's Third Law, results in a force on the particle inwards into the hole, trapping the particle. The light transmission can be monitored; hence, the trap can become a sensor. The SIBA trapping technique can be further improved by using a double-nanohole structure.

The double-nanohole structure has been shown to give a strong local field enhancement[5,6]. Between the two sharp tips of the double-nanohole, a small particle can cause a large change in optical transmission, thereby inducing a large optical force. As a result, smaller nanoparticles can be trapped, such as 12 nm silicate spheres[7] and 3.4 nm hydrodynamic radius bovine serum albumin proteins[8]. In this work, the experimental configuration used for nanoparticle trapping is outlined. First, we detail the assembly of the trapping setup which is based on a Thorlabs Optical Tweezer Kit. Next, we explain the nanofabrication procedure of the double-nanohole in a metal film, the fabrication of the microfluidic chamber and the sample preparation. Finally, we detail the data acquisition procedure and provide typical results for trapping 20 nm polystyrene nanospheres.

Video Link

The video component of this article can be found at http://www.jove.com/video/4424/

Protocol

The principle of the SIBA trapping technique is illustrated in **Figure 1**. **Figure 2** is a schematic of the experimental setup.

1. Optical Trapping Setup

For this section of the procedure, refer to the optical trapping kit manual[9] or the optical force measurement module manual[10] for details on setting up the kits. Note that an avalanche photodiode (APD) is used instead of a quadrant position detector. For screws not included in the optical trapping kit, use the ones in the cap screw and hardware kit (Thorlabs, HW-KIT2). Eye protection should be worn at all times when the laser is on. Make sure the beam is contained within a safe area and reflective accessories, such as jewelry, should be avoided. Also, electrostatic discharge protection is advisable when handling laser diodes.

1. Set up the optical tweezer kit (Thorlabs, OTKB/M) and the force measurement module (Thorlabs, OTKBFM) as per their respective manuals. A silicon-based avalanche photodiode (APD) (Thorlabs, APD110A) is used instead of the force measurement module's (Thorlabs, OTKBFM) quadrant position detector.
2. Connect the APD to an oscilloscope (Tektronics, TDS1012) via a coaxial cable.
3. Add a half-wave plate (Thorlabs, AHWP05M-980) inside the beam expander. The half-wave plate is fastened between two lens tubes (Thorlabs, SM1L03).

2. Nanofabrication

1. Cut a gold-coated test slide (EMF Corp, Cr/Au) into four identical pieces. As an alternative to the commercially available slides, we have also used a 100 nm thick Au film with a 2 nm Ti adhesion layer deposited by e-beam deposition onto a 1 inch square glass slide at an elevated substrate temperature of 200 °C for at least 1 hr. This produces a smooth polycrystalline film.
2. Create a bitmap image of the double-nanohole structure as the input to the focused ion beam (FIB) system is a bitmap. The image consists of two solid circles, 160 nm in diameter with a center to center distance of 190 nm. This template creates a tip separation of approximately 15 nm. Between the circles, an optional thin line can be placed to remove any residue metal in between the tips. **Figure 3a** shows an example bitmap image.
3. Fabricate the double-nanohole structure using a FIB (Hitachi, FB-2100) milling system. Convert the bitmap in step 2.2 into a FIB milling pattern (the dark area in the bitmap gets milled by the FIB). Use an ion accelerating voltage of 40 kV, a beam limiting aperture of 15 µm diameter under 60 K times magnification. Mill eighty passes for each double-nanohole with a 5 µsec dose time on each pass. **Figure 3b** shows a typical resulting structure. Repeat as needed. Multiple nanoholes should be made as to allow for errors.
4. Add registration markers, either using the FIB and/or by hand to indicate the approximate location of the double-nanohole(s).
5. Optionally, take a SEM image of the holes to accurately evaluate structure quality and tip separation.

3. Microfluidic Chamber

A process flow diagram for fabricating the microfluidic chamber is shown in **Figure 4**.

1. Pour 10 g of polydimethylsiloxane (PDMS) base (Dow Corning Canada, Sylgard 184 Silicone Elastomer Base) and an additional 1 g of curing agent (Dow Corning Canada, Sylgard 184 Silicone Elastomer Curing Agent) into a disposable cup. Mix for a few minutes.
2. Evacuate mixture in vacuum chamber until all bubbles are gone.
3. Pour 1.5 g of PDMS into a 9 cm diameter Petri dish. Spin coat PDMS on the bottom of Petri dish at 950 rpm for 65 sec. **Figure 4b** shows the result. The thickness is not critical as long as it is under 80 µm; the gold film is within the bottom microscope objective's working distance.
4. Gently place 3-5 #1.5 coverslips (Fisher Scientific, 12-541-B) onto the PDMS such that they do not overlap and evacuate for 30 min as shown in **Figure 4c**.
5. If coverslips moved and stacked one on top of each other during evacuation, gently move them off each other. Caution must be taken as to keep PDMS under coverslips thin and uniform.
6. If manipulation of coverslips was required, evacuate Petri dish again for 30 min.
7. Remove Petri dish from vacuum chamber and cook on hot plate for 20 min at 85 °C.
8. Using a razor blade, cut out one of the cover slips then gently pry up the slide using fine tip tweezers. A thin layer of PDMS will stay on the coverslip as PDMS is more adhesive to the glass cover slip than the PMMA Petri dish as in **Figure 4e**.
9. Cut out a 3 x 3 mm window in the PDMS with a razor blade as in **Figure 4f**. This window will form the chamber where the nanoparticle solution will be kept.

4. Sample Preparation

1. Fabricate a microscope slide with a ¾" diameter hole at the center using acrylic. This can be accomplished with a laser cutter. Other materials can be used as well. The gold sample will be placed inside the hole.
2. Tape the circumference of the hole with double sided tape. Use a razor blade to cut excess tape.
3. Place microscope slide on to the coverslip, PDMS face up.
4. Dilute the polystyrene nanosphere solution (Thermo Scientific, 3020A) from 1 % w/v to 0.05 % w/v using deionized water. A micropipette can be used.
5. Add a few drops of solution in the PDMS window. Add a drop onto the gold sample where the nanoholes are located.
6. Place gold sample on top of coverslips such that the nanoholes are inside the PDMS window. Make sure bubbles are not present inside chamber. Press gold sample against coverslip and dab any excess solution.
7. If using an oil immersion objective (as is the case here, but not necessary), add a drop of immersion oil on the opposite side of the coverslip, underneath the PDMS window. Take note of the location of the nanoholes.
8. Insert microscope slide into slide holder, oil facing down, and then lower slide holder until immersion oil makes contact with the microscope objective.
9. Roughly align slide stage such that indicator marks are underneath the objective.
10. Follow indicator lines leading up to the nanoholes. Position slide such that indicator marks and other open areas are cleared from the screen center. Excessive light transmission can damage the APD.
11. Turn on laser. As the dichroic mirror is not perfect, a spot near the center of the screen from the laser beam should appear.
12. Using the piezo stage control software, further refine the alignment on all three axes.

5. Data Acquisition

1. With the help of the indicator marks, position the spot close to a known nanohole location. The nanoholes will be too small to be resolved and should appear only as spots.
2. The light transmission through the sample is indicated by the signal level on the oscilloscope. Further align the sample as to maximize light transmission. Be careful of indicator marks and visible and non-visible scratches as light transmission will be high in these areas. Nanoholes will show sudden jumps in light transmission while scratches exhibit more gradual changes.
3. Using the waveplate, adjust the light polarization for highest light transmission as the double-nanohole structure is polarized.
4. To minimize noise, build an RC filter with the breadboard, 200 KΩ resistor and 100 pF capacitor and connect it after the APD via a coaxial cable. These values can be adjusted for best performance, considering the bandwidth of data acquisition required.

5. Connect oscilloscope and data acquisition module (Omega, USB-4711A) to the RC filter with coaxial cables and T adapter.
6. Sample the APD's voltage using the data acquisition module for the desired time. Acquisition times are typically in the hundreds of seconds. In this case, a custom software package was used for data acquisition. The voltage is sampled at 2,000 times per second.
7. Using Matlab, filter the acquired data using a Savitzky-Golay filter and plot it versus time on a graph.

Representative Results

A typical acquisition trace is shown in **Figure 5a**. A trapping event is characteristically sudden, with a sharp edge, showing a clear switch between two transmission power levels. As particles are subject to Brownian motion, the trapping events will occur randomly. For 20 nm particles, transmission changes from trapping were typically around 5-10 % and trapping times, around 10-300 sec. The typical time to achieve a trapping event for the power and concentration outlined above is on the order of a minute. Due to steric hindrance it is uncommon to see multiple particle trapping simultaneously, although once a particle is released, it is typically followed by a subsequent trapping event. Depending on the quality of the results, there may be some increase in signal noise in the trapped state. This noise increase comes from the Brownian motion of the trapped particle. Without the trapped particle, this noise source is not present.

Some artifacts may show up in the results which are not indicative of trapping events. Results showing drifting, slow changes in the transmission over a period of minutes as shown in **Figure 5b**, should be discarded. Other artifacts may also be present such as inconsistent transmission changes, excessive noise or no trapping at all. For example, bubbles can cause discontinuous intensity jumps if care is not taken to ensure that the chamber is bubble-free. These bubbles will respond differently to the trapping events in terms of dynamic behavior and intensity change, and so they are readily identifiable. Such symptoms could be caused by a poor double-nanohole structure, contaminants or mechanical vibrations. A quiet, low-activity setting is highly recommended to place this setup. Also, allowing laser and stage to settle a few minutes after aligning can help as well.

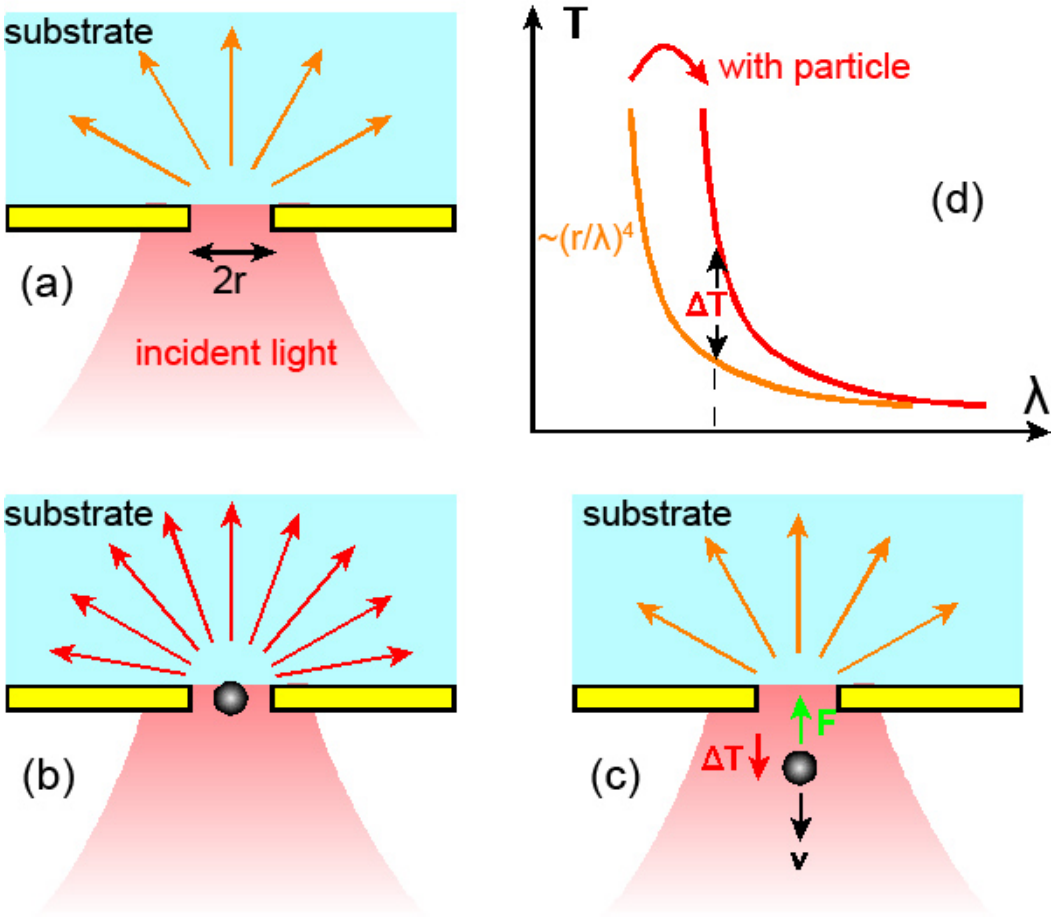

Figure 1. Subwavelength aperture optical transmission: a) Without particle; b) Increased transmission due to dielectric particle; c) If particle attempts to leave, the decrease in light momentum (ΔT) will cause a force (F) on the particle as to pull it back into the hole; d) Red-shifting of the transmission curve caused by the particle, leading to the change in transmission ΔT.

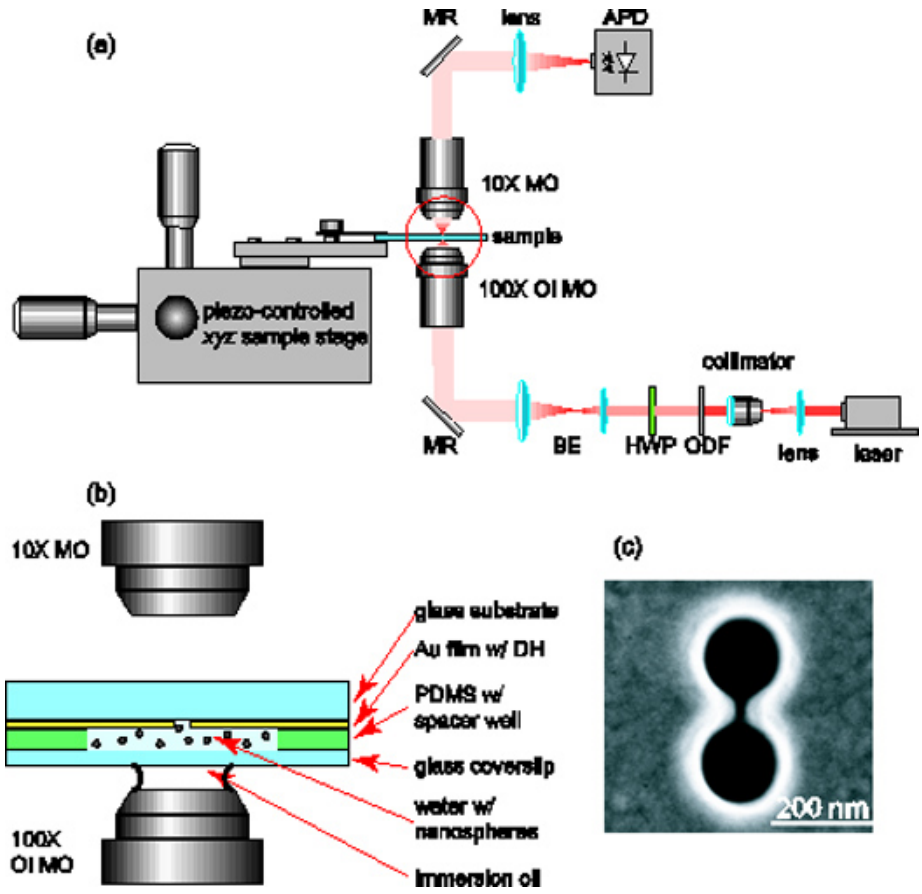

Figure 2. a) Overall schematic of trapping setup, enlargement of red circle is shown in b); b) Enlargement showing the double-nanohole, and the nanospheres inside the PDMS chamber; c) SEM image of the double-nanohole structure. Acronyms used: LD = laser diode; ODF = optical density filter; HWP = half-wave plate; BE = beam expander; MR = mirror; MO = microscope objective; OI MO = oil immersion microscope objective; DH = double-nanohole; APD = avalanche photodetector.

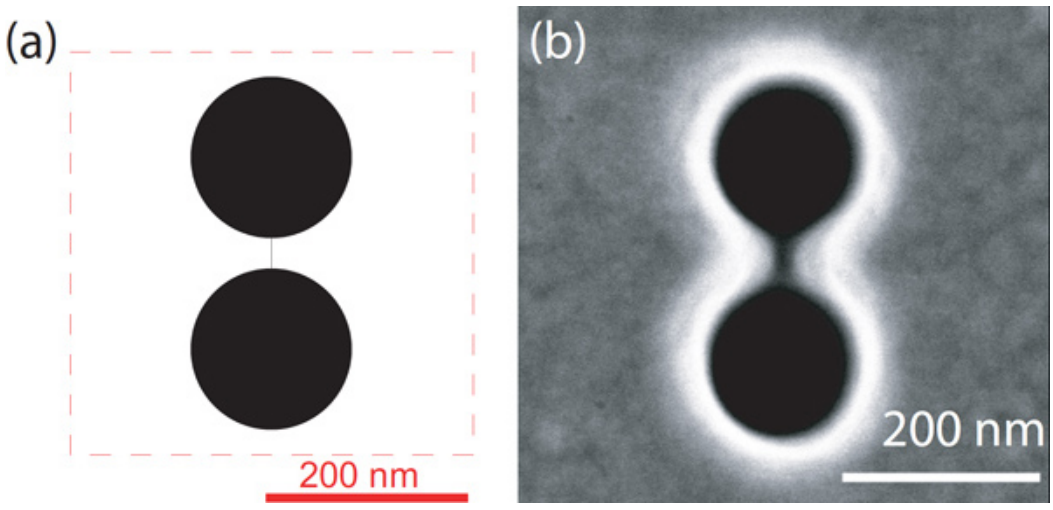

Figure 3. a) Example bitmap figure used in the FIB fabrication; b) A SEM image of a double-nanohole.

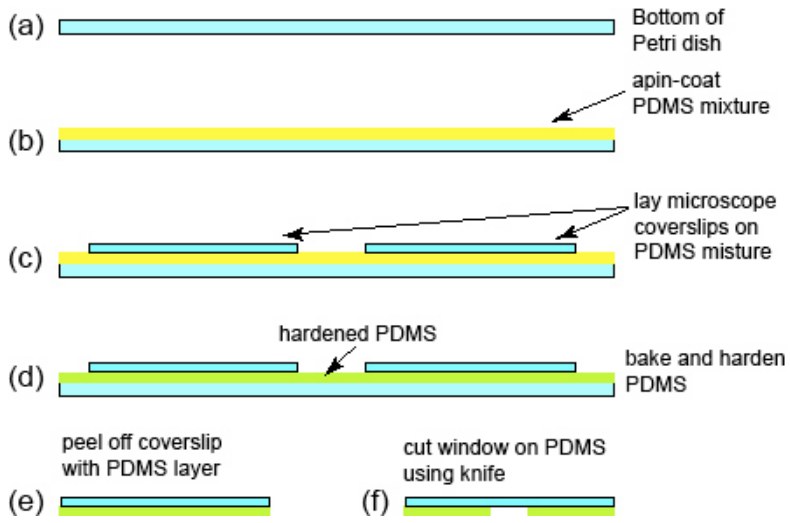

Figure 4. Process diagram for fabricating the microfluidic chamber.

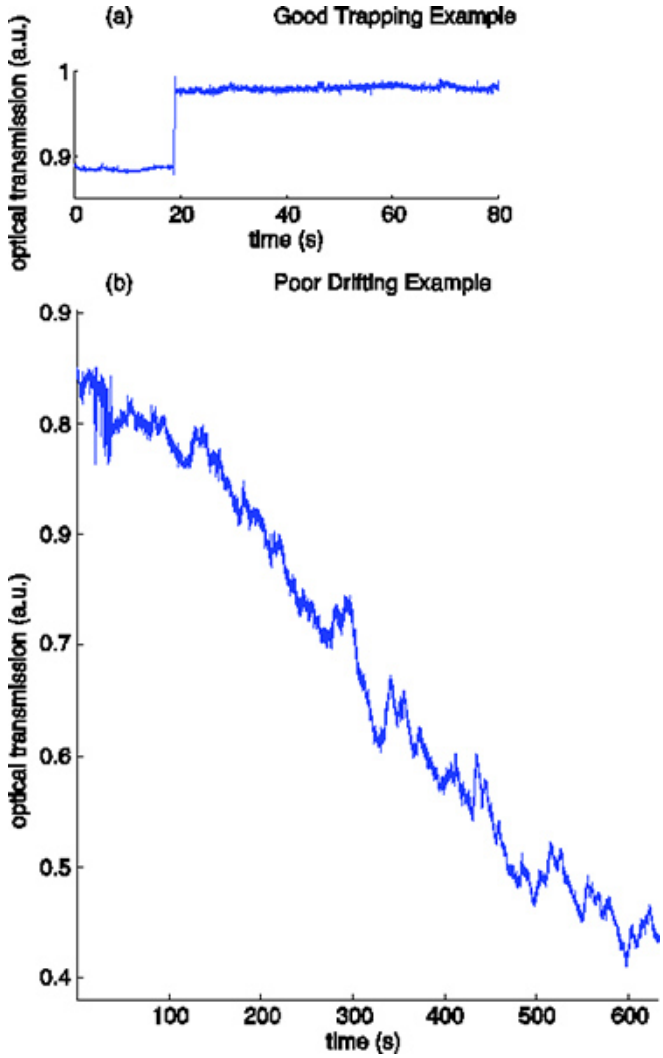

Figure 5. (a) Typical acquisition of trapping events with 20 nm polystyrene spheres. (b) A poor acquisition showing acute drifting.

Discussion

The current setup has effective trapping abilities owing to the structure of the nanohole. This nanohole traps ~10 nm-scale dielectric particles at low optical intensities. Other novel optical traps include optical dipole antennas[11], whispering-gallery-mode optical resonators[12,13] and waveguides[14]; however, they typically operate in the perturbative regime, which is limited by the inverse fourth order scaling of the required optical power versus particle size, unlike the SIBA and double-nanohole trap. Alternative aperture shapes have also been presented for trapping, such as a rectangular plasmonic nanopore[15]. Other favorable qualities shown by the double-nanohole trap include particle size-selective behavior[7], a single trapping location (to limit multi-particle trapping) and ease of fabrication[16]. As an alternative to using a FIB, double-nanoholes can be fabricated by using a colloidal lithography[6].

Trapping of biological materials of large polarizability and size has included bacteria[3], living cells[17,2,18], the tobacco mosaic virus[3] and manipulation and stretching of DNA strands tethered at the ends with large dielectric particles[19]; however, direct trapping of smaller biological samples without tethering remains challenging. This trapping configuration is capable of trapping small dielectric particles at lower light intensities than conventional light tweezers and the circular nanohole, allowing small biological particles to be held for long periods of time without damage or tethering. Also, the trapping events exhibit a high signal-to-noise ratio allowing this setup to work as a sensitive sensor and detect the smallest biological particles, such as viruses and proteins. In fact, 20 nm polystyrene spheres have a refractive index of 1.59 which is comparable to the smallest biological particles such as viruses. This method could become a reliable and mature technique for immobilization and manipulation of nanoparticles, including biological particles.

Applications of this technique include integration into a microfluidic environment. Instead of a single microfluidic chamber, a channel would be used to dynamically control the environment, ideal for refractive index sensing. Such a setup would be set in a single microfluidic chip leading to a more stable and robust setup and faster analysis of solutes. Another option is development of a fluorescence detection scheme for characterization of single fluorescent-tagged viruses, semiconductor quantum dots and green fluorescent proteins. This setup also has potential for modification into a biosensor for a single virus or protein, allowing very small samples to be analyzed. Drug discovery[21] and disease and infection detection[22] would benefit from a single protein detector. Raman spectroscopy can be incorporated for detection of Raman signals of particles and single binding events. The double-nanohole structure allows strong local field enhancements at the tips, appropriate for tip-enhanced Raman spectroscopy[23]. A highly specific label-free method of material characterization would also be possible using Raman spectroscopy[24].

Disclosures

Production and Free Access to this article is sponsored by Thorlabs.

Acknowledgements

We acknowledge Thorlabs for sponsoring this publication and funding from the Natural Science and Engineering Research Council (NSERC) of Canada Discovery Grant. We thank Bryce Cyr and Douglas Rennehan for production assistance in the making of this video article.

References

1. Ashkin, A., Dziedzic, J.M., Bjorkholm, J.E., & Chu, S. Observation of a single-beam gradient force optical trap for dielectric particles. *Opt. Lett.* **11**, 288-290 (1986).
2. Liu, Y., *et al.* Evidence for localized cell heating induced by infrared optical tweezers. *Biophys. J.* **68**, 2137-2144 (1995).
3. Ashkin, A. & Dziedzic, J.M. Optical trapping and manipulation of viruses and bacteria. *Science.* **235**, 1517-1520 (1987).
4. Juan, M.L., Gordon, R., Pang, Y., Eftekhari, F., & Quidant, R. Self-induced back-action optical trapping of dielectric nanoparticles. *Nature Phys.* **5**, 915-919 (2009).
5. Jin, E.X. & Xu, X.F. Enhanced optical near field from a bowtie aperture. *Appl. Phys. Lett.* **88**, 153110 (2006).
6. Onuta, T.-D., Waegele, M, DuFort, C.C., Schaich, W.L., & Dragnea, B. Optical field enhancement at cusps between adjacent nanoapertures. *Nano Lett.* **7**, 557-564 (2007).
7. Pang, Y. & Gordon, R. Optical trapping of 12 nm dielectric spheres using double-nanoholes in a gold film. *Nano Lett.* **11**, 3763-3767 (2011).
8. Pang, Y. & Gordon, R. Optical trapping of a single protein. *Nano Lett.* **12**, 402-406 (2012).
9. Optical trap kit - Manual. http://www.thorlabs.com/thorcat/19900/OTKB_M-Manual.pdf, (2011).
10. Optical trap kit - The force module. http://www.thorlabs.com/thorcat/19500/OTKBFM-Manual.pdf, (2011).
11. Righini, M., *et al.* Nano-optical trapping of rayleigh particles and *escherichia coli* bacteria with resonant optical antennas. *Nano Lett.* **9**, 3387-3391 (2009).
12. Arnold, S., *et al.* Whispering gallery mode carousel - a photonic mechanism for enhanced nanoparticle detection in biosensing. *Opt. Express.* **17**, 6230-6238 (2009).
13. Lin, S., Schonbrun, E., & Crozier, K. Optical manipulation with planar silicon microring resonators. *Nano Lett.* **10**, 2408-2411 (2010).
14. Yang, A.H.J., *et al.* Optical manipulation of nanoparticles and biomolecules in sub-wavelength slot waveguides. *Nature.* **457**, 71-75 (2009).
15. Chen, C., *et al.* Enhanced optical trapping and arrangement of nano-objects in a plasmonic nanocavity. *Nano Lett.* **12**, 125-132 (2012).
16. Lyer, S., Popov, S., & Friberg, A.T. Impact of apexes on the resonance shift in double hole nanocavities. *Opt. Express.* **18**, 193-203 (2010).
17. Ashkin, A., Dziedzic, J.M., & Yamane, T. Optical trapping and manipulation of single cells using infrared laser beams. *Nature.* **330**, 769-771 (1987).

18. Liu, Y., Sonek, G.J., Berns, M.W., & Tromberg, B.J. Physiological monitoring of optically trapped cells: Assessing the effects of confinement by 1,064 nm laser tweezers using microfluorometry. *Biophys. J.* **71**, 2158-2167 (1996).
19. Wang, M.D., Yin, H., Landick, R., Gelles, J., & Block, S.M. Stretching dna with optical tweezers. *Biophys. J.* **72**, 1335-1346 (1997).
20. Operation manual-apd110x series-avalanche photodiodes. http://www.thorlabs.com/thorcat/19500/APD110A-Manual.pdf, (2011).
21. Yu, D., Blankert, B., Viré, J.C., & Kauffmann, J.M. Biosensors in drug discovery and drug analysis. *Anal. Lett.* **38**, 1687-1701 (2005).
22. Luppa, P.B., Sokoll, L.J., & Chan, D.W. Immunosensors-principles and application to clinical chemistry. *Clin. Chim. Acta.* **314**, 1-26 (2001).
23. Min, Q., Santos, M.J.L., Girotto, E.M., Brolo, A.G., & Gordon, R. Localized raman enhanced from a double-hole nanostructure in a metal film. *J. Phys. Chem. C.* **112**, 15098-15101 (2008).
24. Weber-Bargioni, A., *et al.* Hyperspectral nanoscale imaging on dielectric substrates with coaxial optical antenna scan probes. *Nano Lett.* **11**, 1201-1207 (2011).

